

Mapping the functional yeast ABC transporter interactome

Jamie Snider¹, Asad Hanif^{1,2}, Mid Eum Lee⁵, Ke Jin^{1,2,4}, Analyn R. Yu¹, Chris Graham^{1,6}, Matthew Chuk^{1,2}, Dunja Damjanovic^{1,2}, Marta Wierzbicka¹, Priscilla Tang^{1,2}, Dina Balderes⁷, Victoria Wong¹, Matthew Jessulat⁶, Katelyn D. Darowski^{1,3}, Bryan-Joseph San Luis^{1,2,4}, Igor Shevelev¹, Stephen L Sturley⁷, Charles Boone^{1,2,4}, Jack F. Greenblatt^{1,2,4}, Zhaolei Zhang^{1,2,4}, Christian M. Paumi⁸, Mohan Babu⁶, Hay-Oak Park⁵, Susan Michaelis⁹ and Igor Stagljjar^{1,2,3*}

¹ Donnelly Centre, University of Toronto, ON, Canada

² Department of Molecular Genetics, University of Toronto, ON, Canada

³ Department of Biochemistry, University of Toronto, ON, Canada

⁴ Banting and Best Department of Medical Research, University of Toronto, ON, Canada

⁵ Department of Molecular Genetics, the Molecular Cellular Developmental Biology Program, The Ohio State University, Columbus, OH, USA

⁶ Department of Biochemistry, Research and Innovation Centre, University of Regina, Regina, SK, Canada

⁷ Department of Pediatrics, Columbia University Medical Center, New York, NY, USA

⁸ Graduate Center for Toxicology, University of Kentucky, Lexington, KY, USA

⁹ Department of Cell Biology, Johns Hopkins School of Medicine, Baltimore, MD, USA

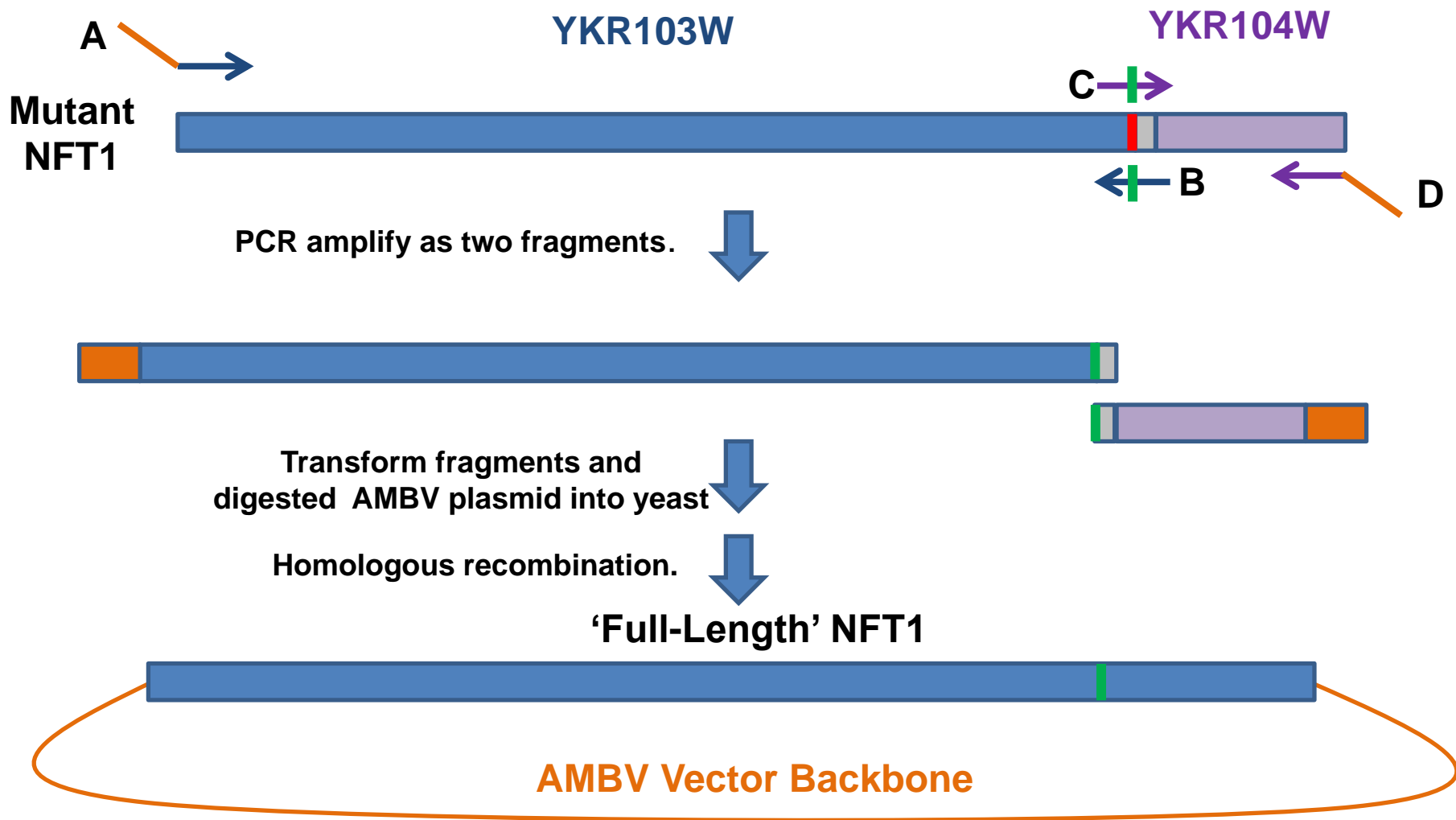
*** Corresponding author**

Email: igor.stagljjar@utoronto.ca

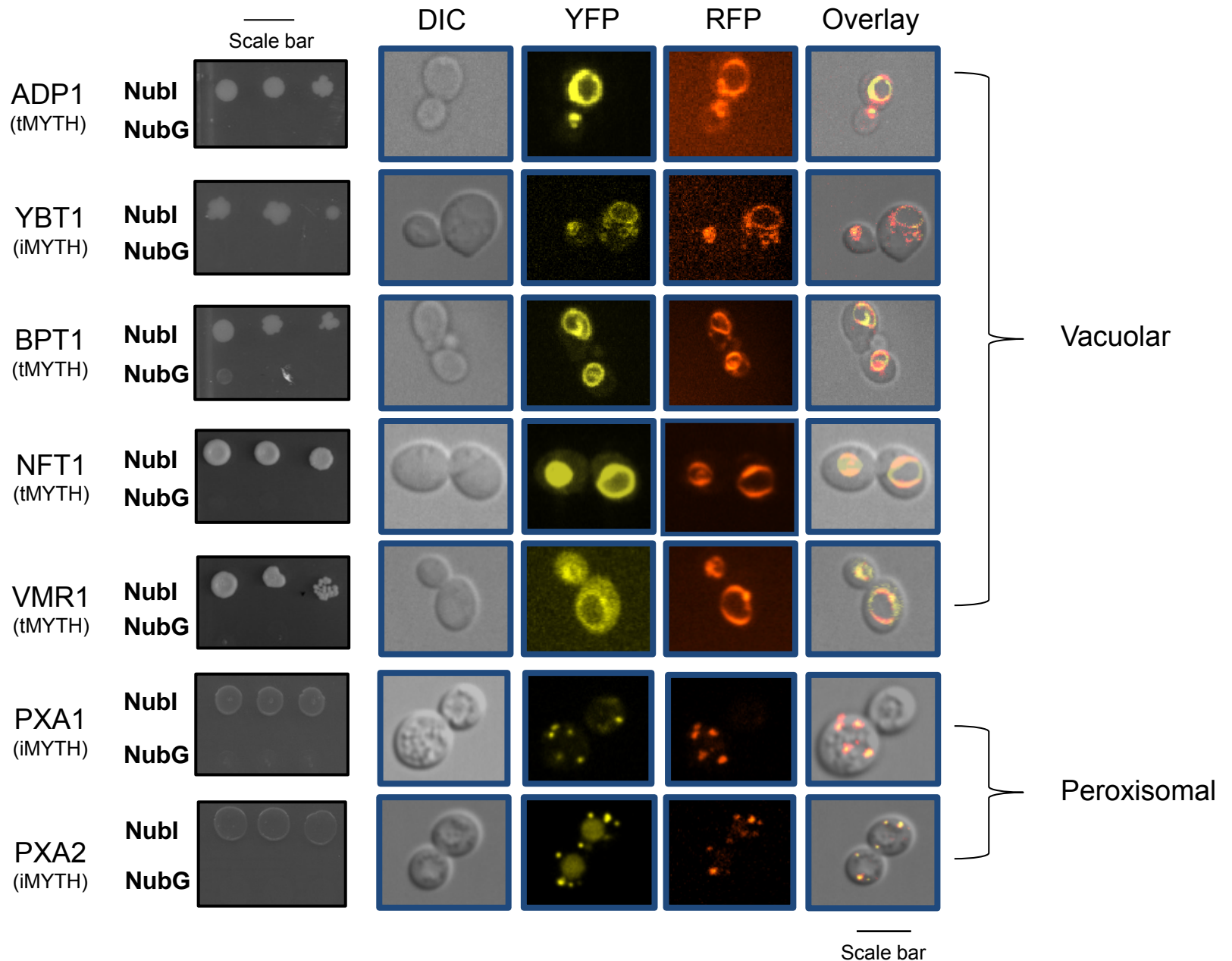
Phone: 1-416-946-7828

Fax: 1-416-978-8287

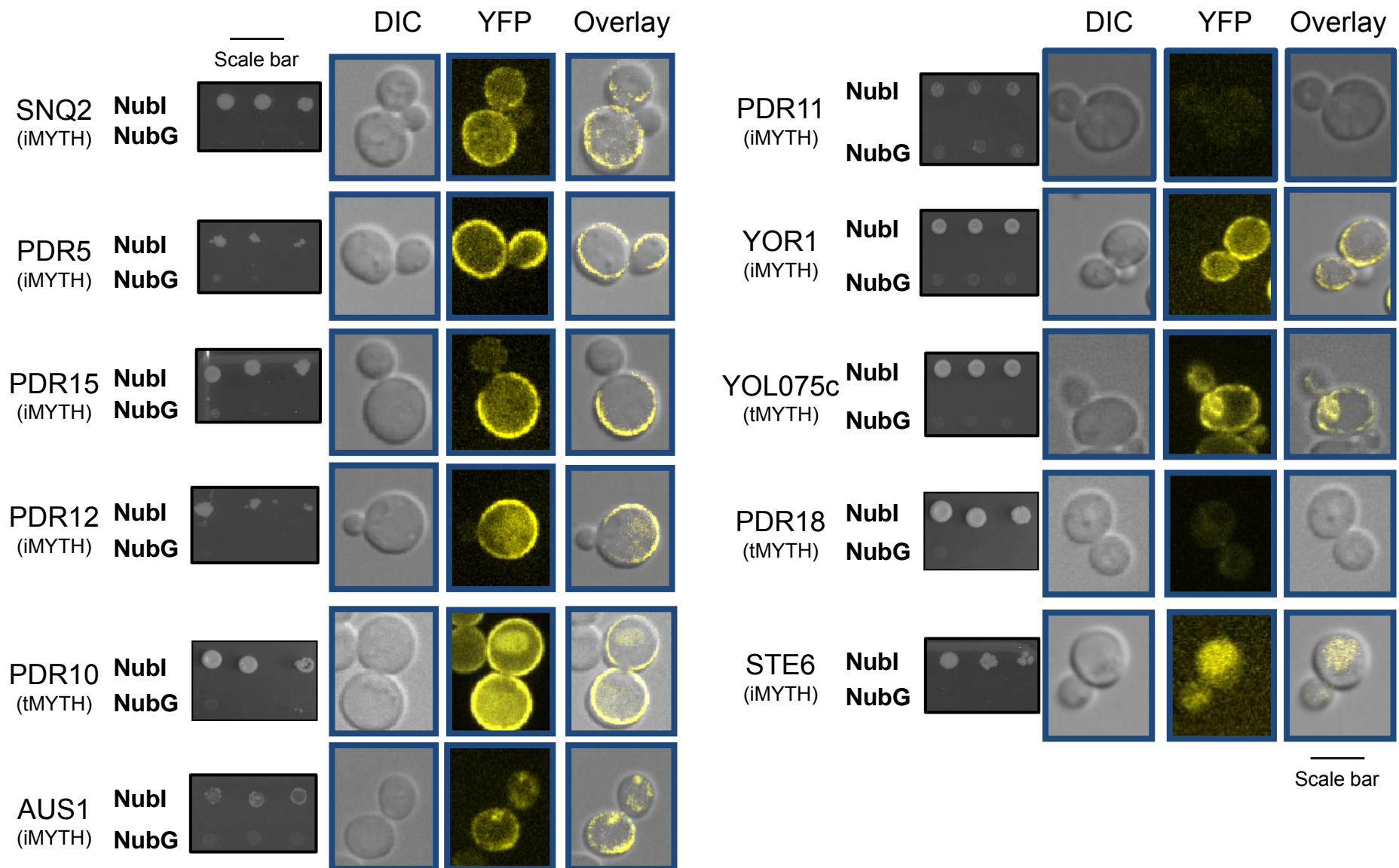
Supplementary Results



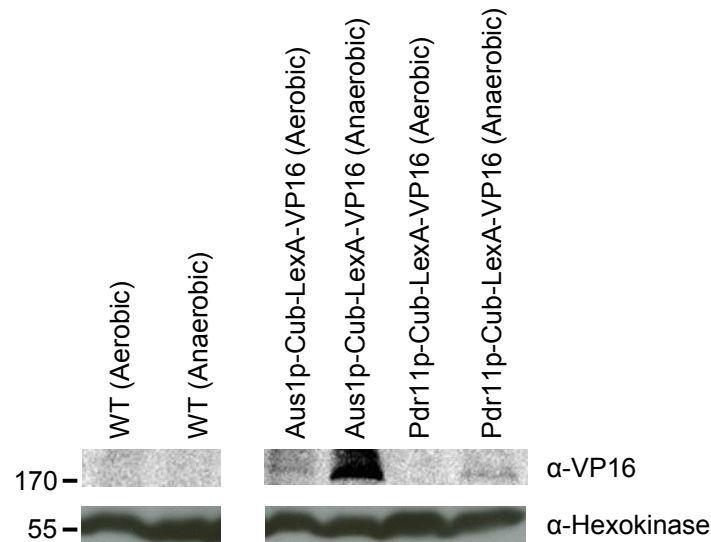
Supplementary Figure 1: Amplification and cloning of 'Full-Length' *NFT1* gene. The mutant *NFT1* gene present in S288C contains a stop codon (TAG) at position 1219 (shown as a Red line) resulting in the annotation of *NFT1* as two separate open reading frames in the SGD – *YKR103W* (Blue) and *YKR104W* (Purple). To repair the mutation, the mutant gene was PCR amplified as two separate fragments using overlapping primers (B and C) which corrected the nonsense mutation and restored the WT 'TAT' codon at position 1219 (shown as a Green line). Both terminal primers (A and D) contained regions homologous to the MYTH AMBV bait vector (shown in Orange). Transformation of both PCR amplified fragments, alongside appropriately digested MYTH AMBV bait plasmid, into yeast, resulted in homologous recombination producing 'Full-Length' WT *NFT1* in the AMBV tMYTH bait vector backbone.



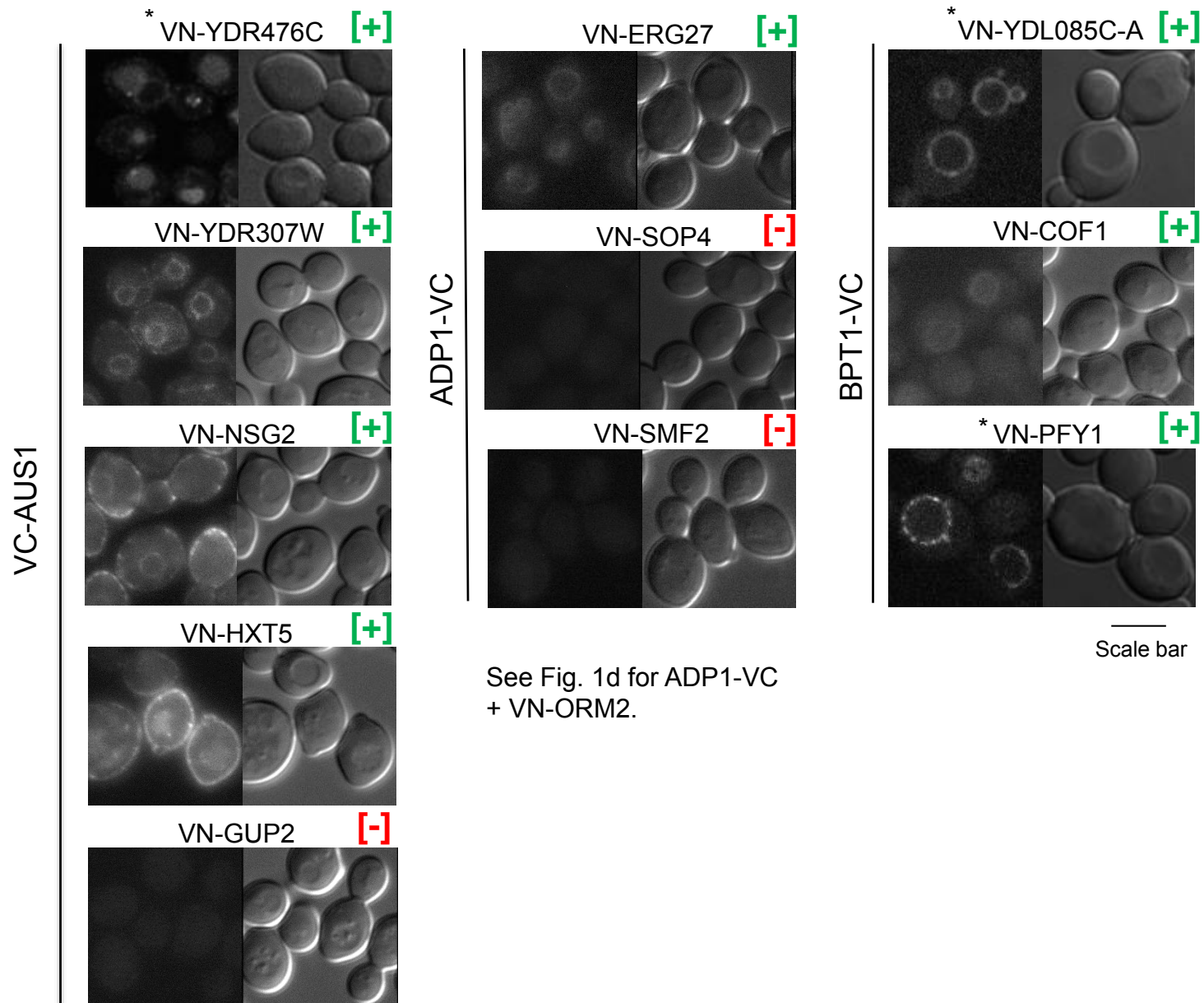
Supplementary Figure 2: NubGI test and fluorescence microscopy subcellular localization results for vacuolar and peroxisomal ABC transporter bait strains used in MYTH screening. Scale bar is 10 mm for NubGI images and 6 μ m for microscopy images.



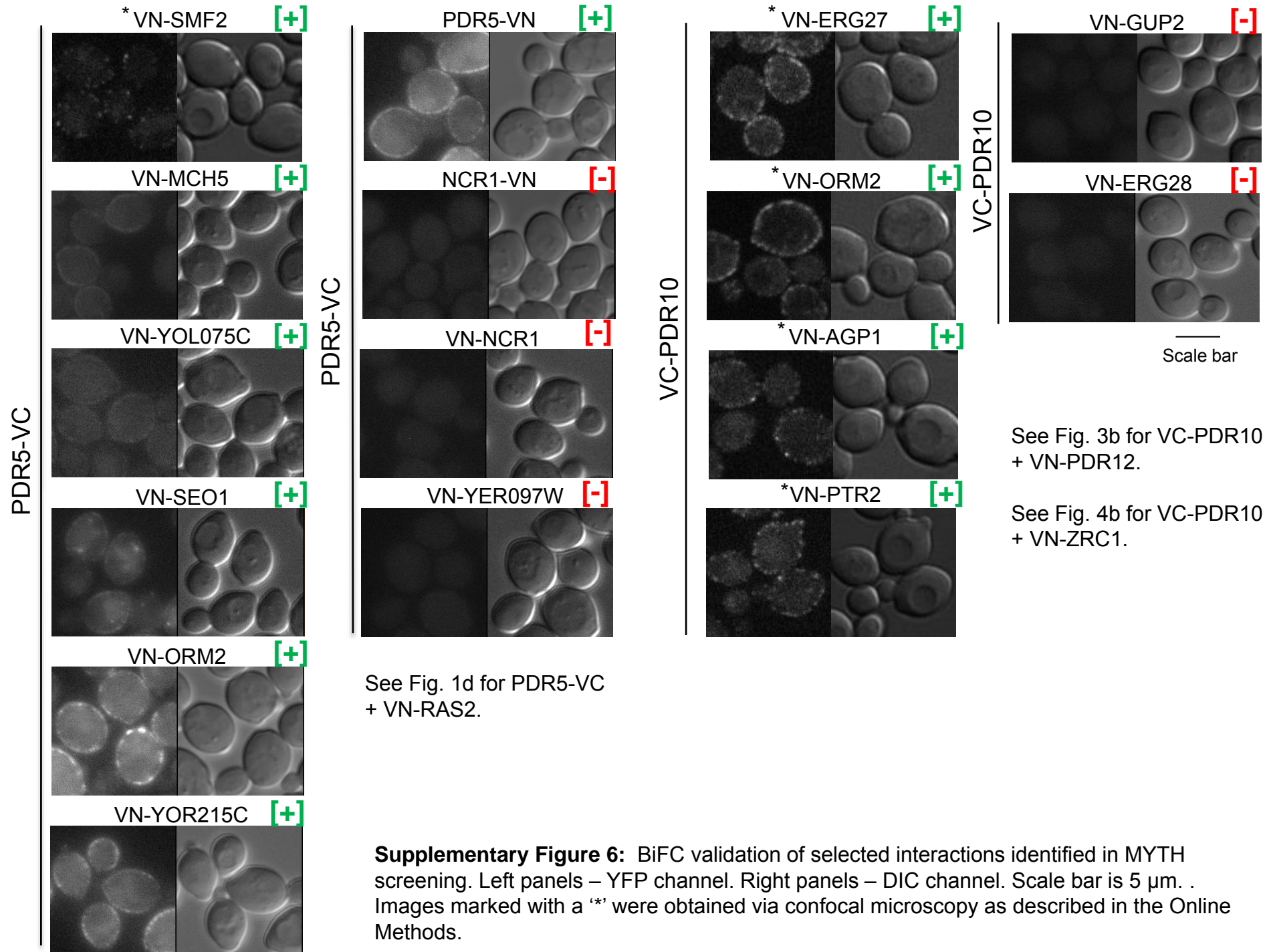
Supplementary Figure 3: NubGI test and fluorescence microscopy subcellular localization results of ABC transporter MYTH baits with predicted plasma membrane localization. Scale bar is 15 mm for NubGI images and 6 μ m for microscopy images. Note that cells expressing Aus1p baits were grown under anaerobic conditions, as described in the Online Methods section.

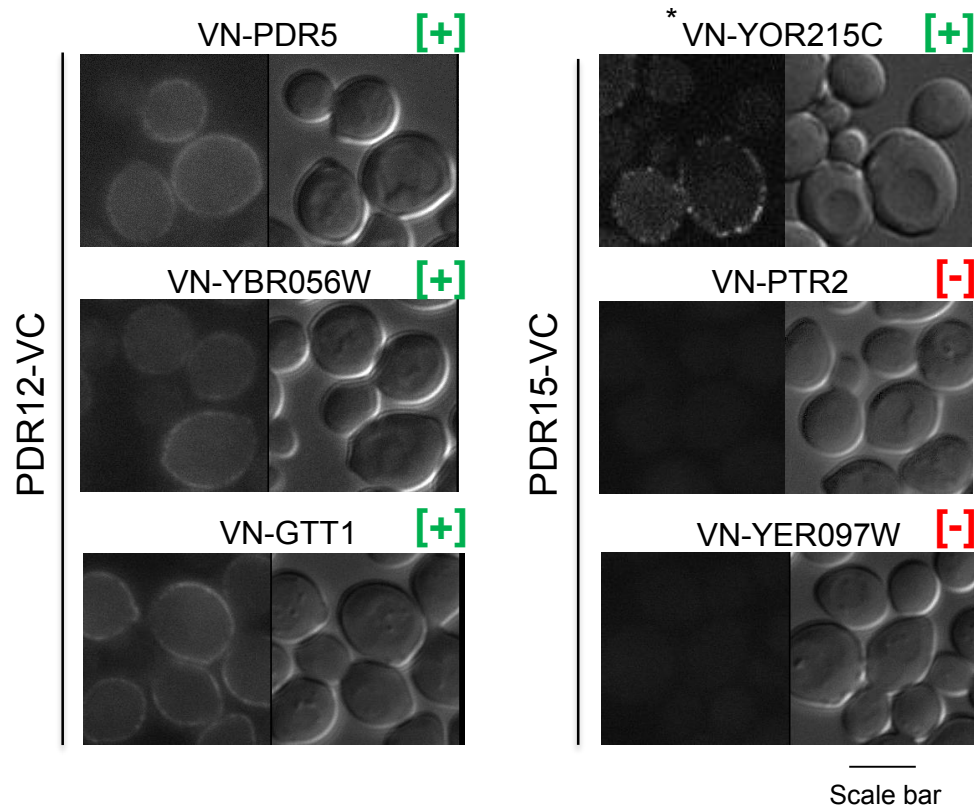


Supplementary Figure 4: Expression of Aus1p and Pdr11p under aerobic and anaerobic growth conditions monitored by Western blot. MYTH-tagged Aus1p and Pdr11p protein levels were measured using antibody directed against the VP16 moiety of the MYTH tag. WT cells, not expressing MYTH-tagged protein, were used as a negative control. Hexokinase levels were monitored in all cases to ensure equal loading.



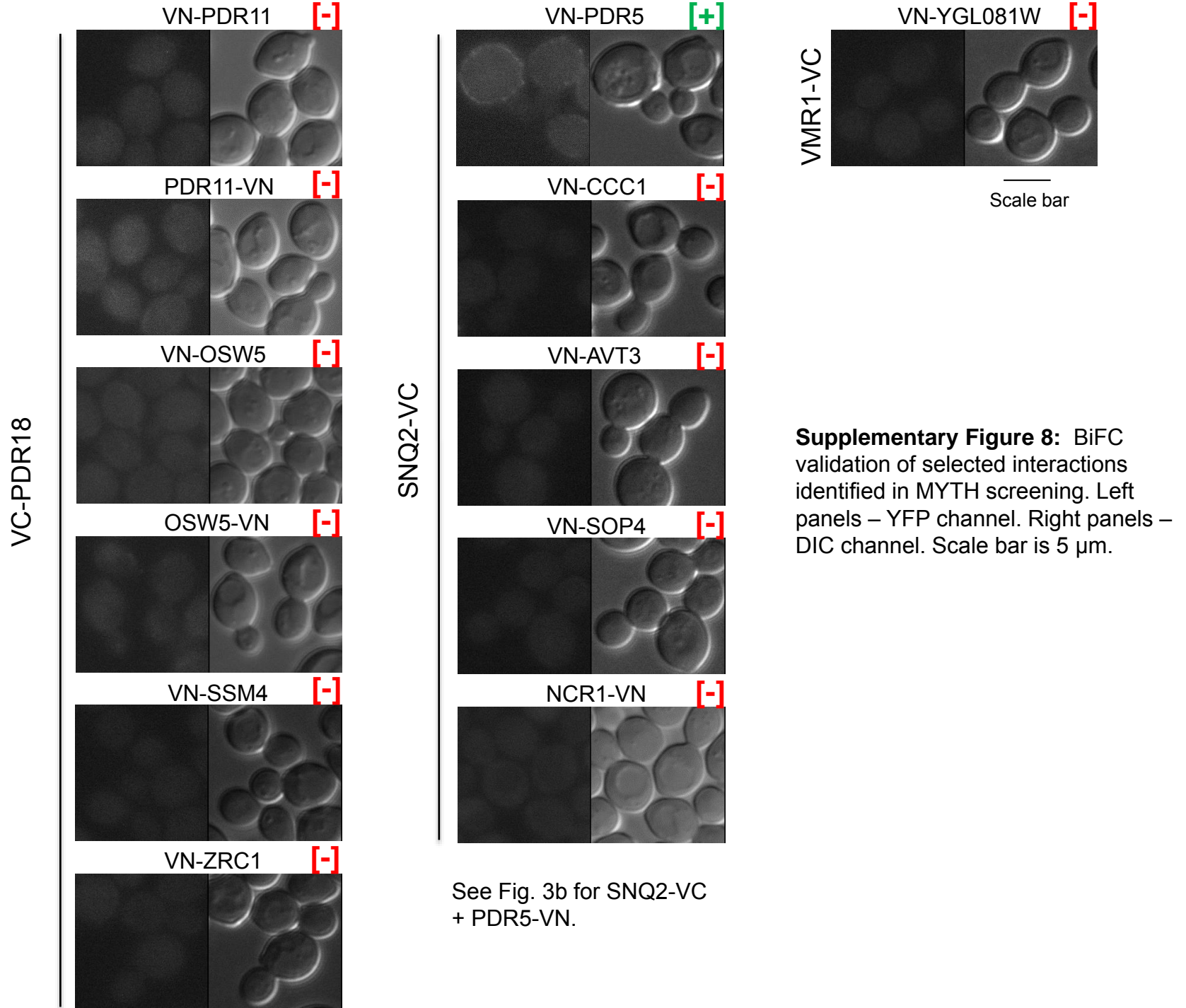
Supplementary Figure 5: BiFC validation of selected interactions identified in MYTH screening. Left panels – YFP channel. Right panels – DIC channel. Scale bar is 5 μ m. Images marked with a ‘*’ were obtained via confocal microscopy as described in the Online Methods.

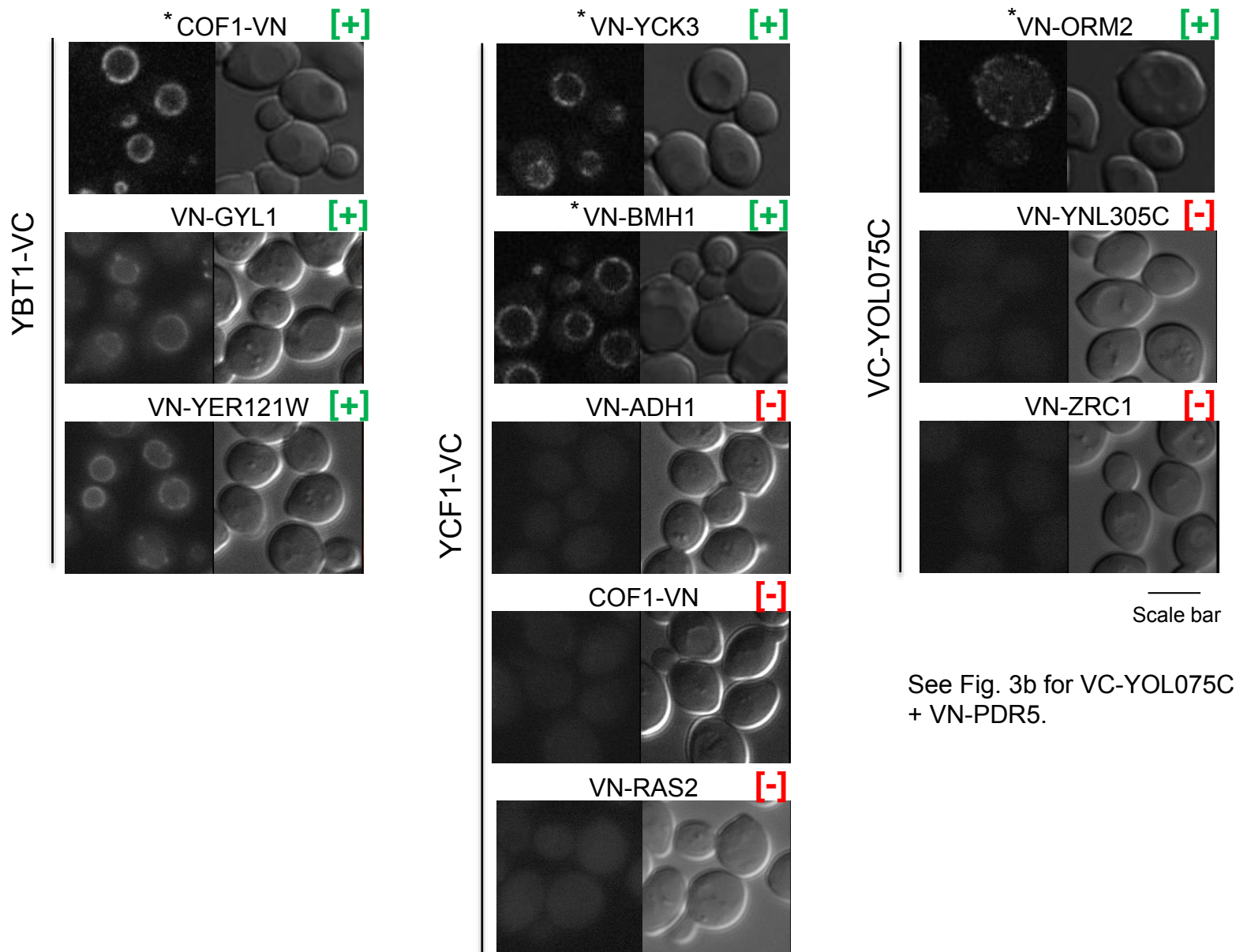




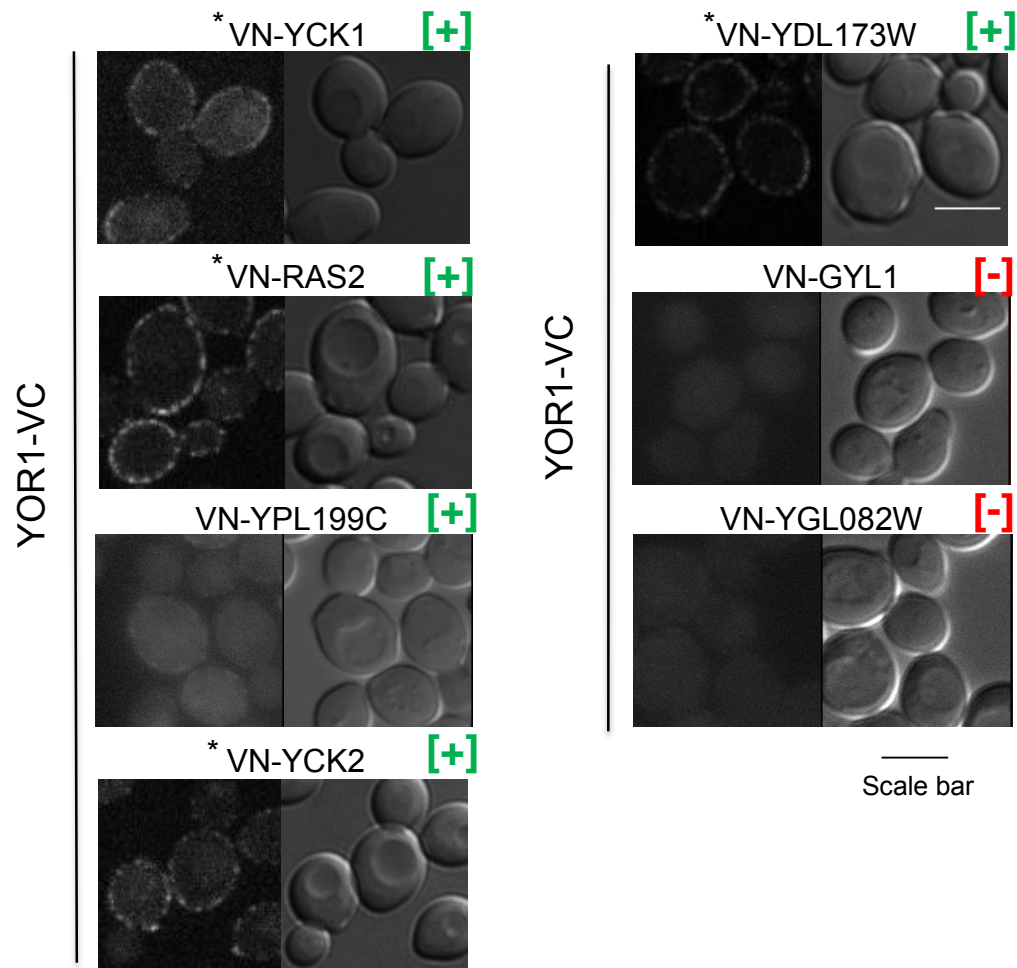
See Fig. 3b for VC-PDR11
Images.

Supplementary Figure 7: BiFC validation of selected interactions identified in MYTH screening. Left panels – YFP channel. Right panels – DIC channel. Scale bar is 5 μ m. Images marked with a ‘*’ were obtained via confocal microscopy as described in the Online Methods.



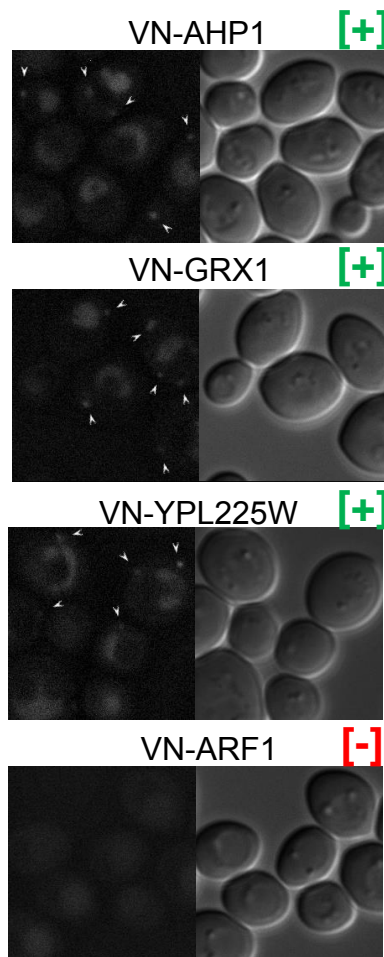


Supplementary Figure 9: BiFC validation of selected interactions identified in MYTH screening. Left panels – YFP channel. Right panels – DIC channel. Scale bar is 5 μ m. Images marked with a ‘*’ were obtained via confocal microscopy as described in the Online Methods.

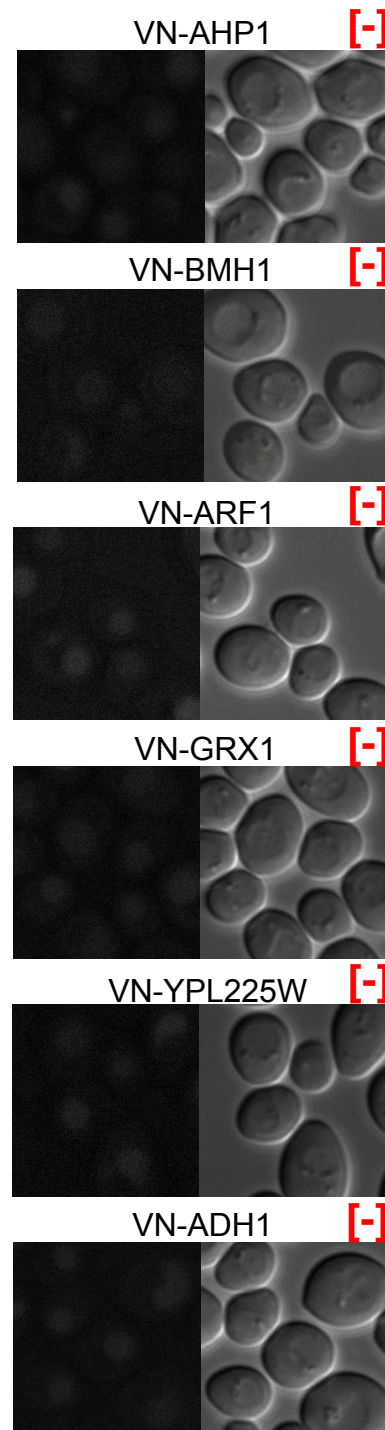


Supplementary Figure 10: BiFC validation of selected interactions identified in MYTH screening. Left panels – YFP channel. Right panels – DIC channel. Scale bar is 5 μ m. Images marked with a “*” were obtained via confocal microscopy as described in the Online Methods.

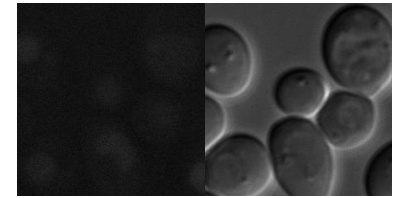
PXA1-VC



VC-PXA2

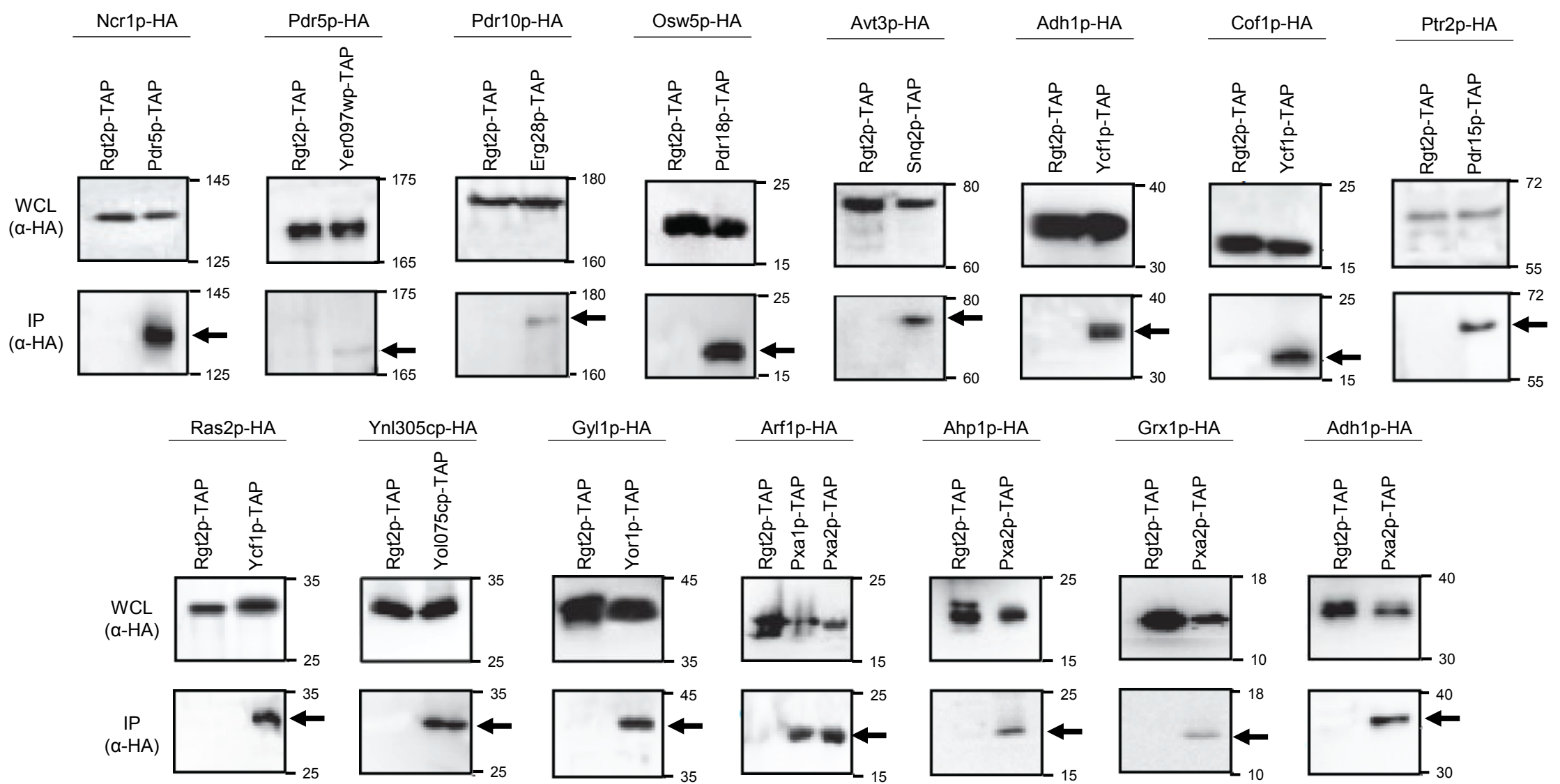


Diploid of BY4741 (Control);
no VN or VC fusions



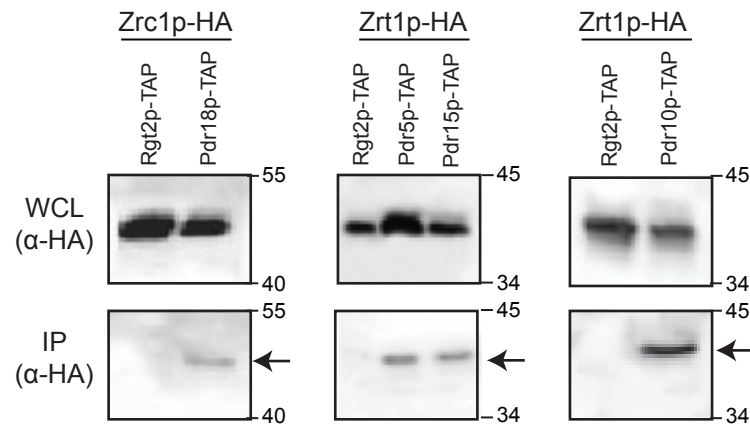
Scale bar

Supplementary Figure 11: BiFC validation of selected interactions identified in MYTH screening. Left panels – YFP channel. Right panels – DIC channel. Arrows in PXA1-VC point to positive punctate signal corresponding to interaction at peroxisomes. Scale bar is 5 μ m.

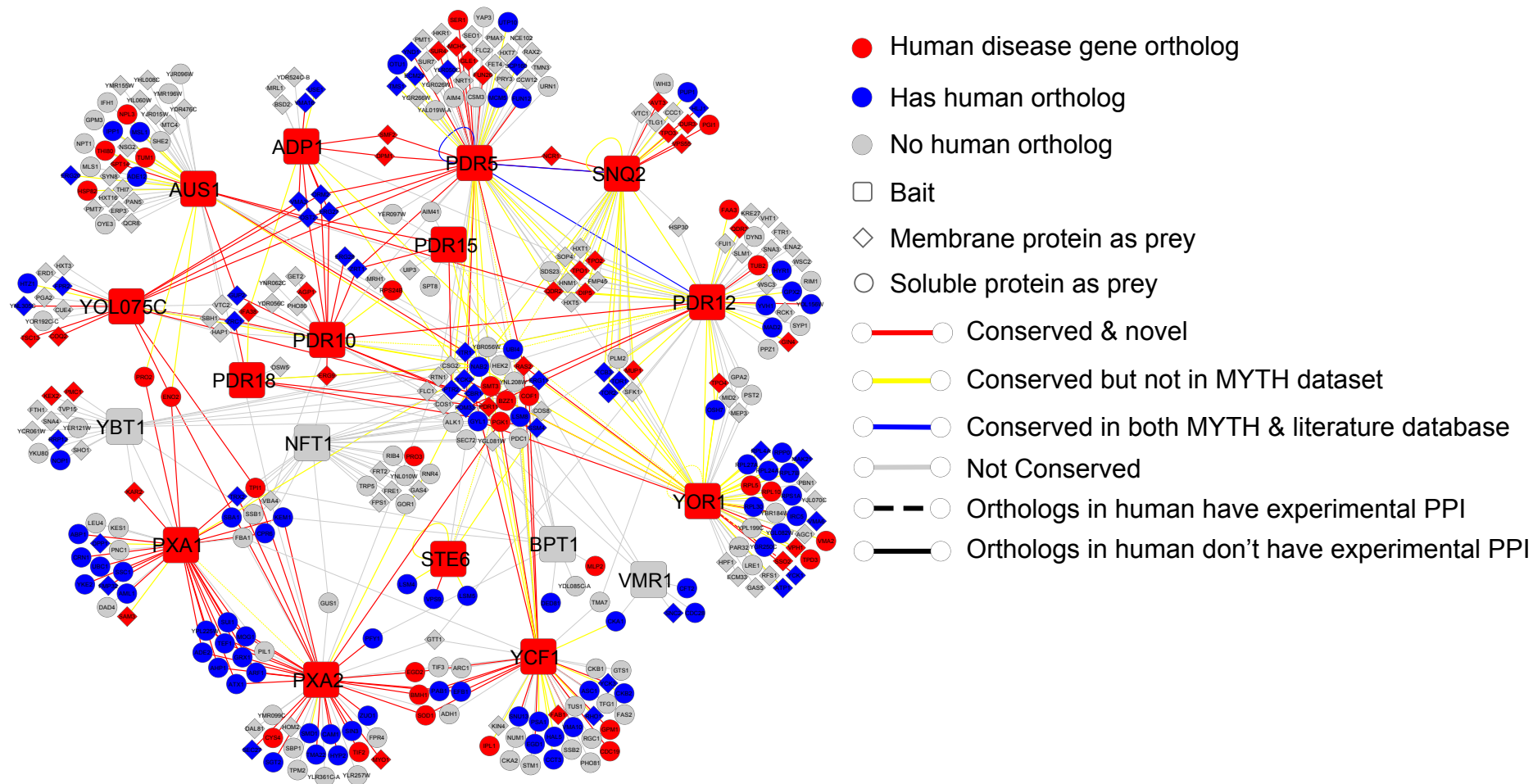


Interactions Not Successfully Validated by Co-IP: Aus1p-Gup2p, Adp1p-Sop4p, Adp1p-Smf2p, Pdr10p-Gup2p, Snq2p-Ccc1p, Snq2p-Sop4p, Snq2p-Ncr1p, Vmr1p-Ygl081wp, Ynl075cp-Zrc1p, Yor1p-Ygl082wp and Pxa2p-Ylp225wp

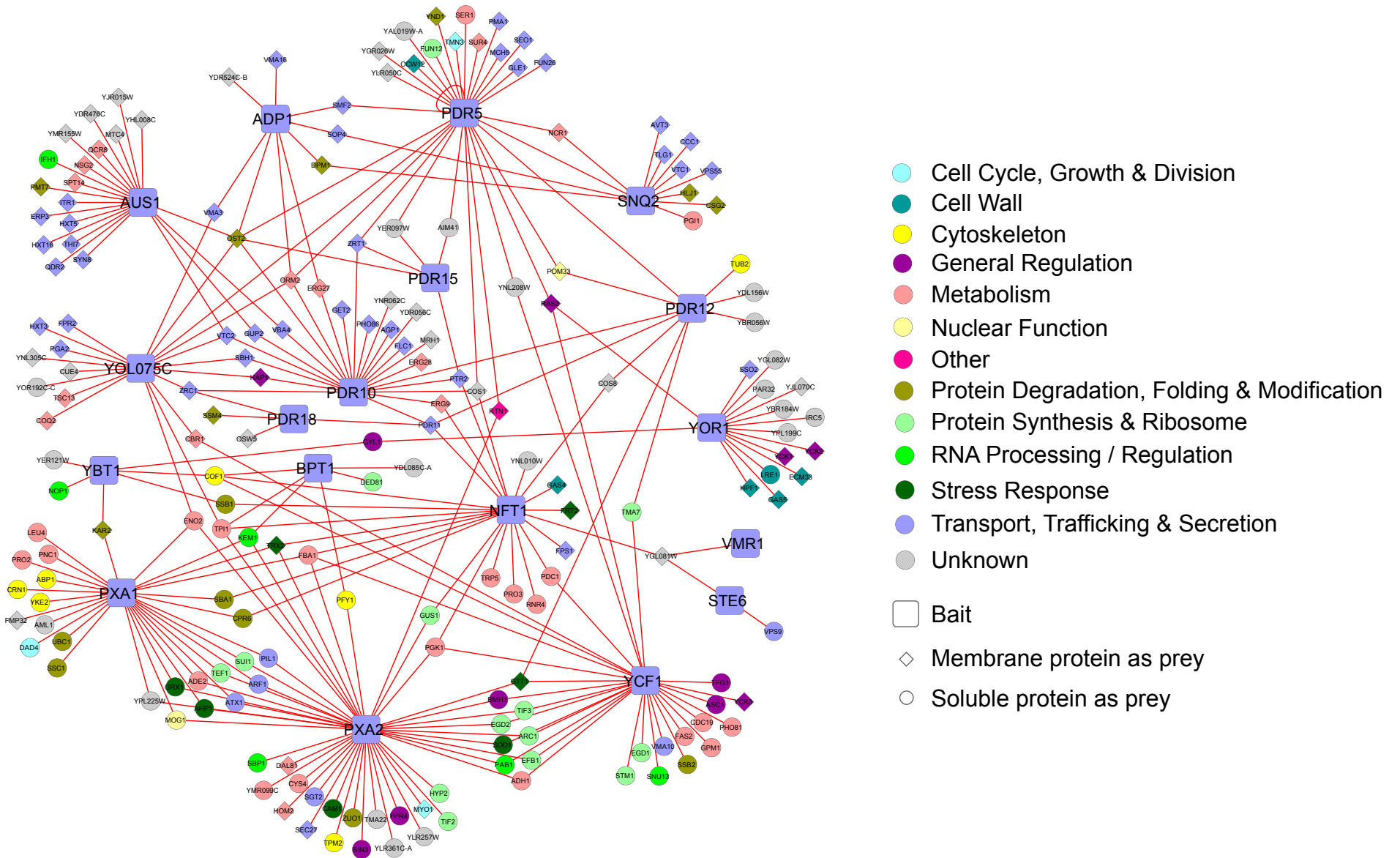
Supplementary Figure 12: Co-immunoprecipitation validation of MYTH interactions which could not be confirmed by BiFC. Sizes indicated at top and bottom of boxes were estimated from MW markers on blots and are given in kDa. Rgt2p-TAP was used as a negative control. Interactions which were not successfully validated by Co-IP are listed in the box below the images. Four interactions (Pdr11p-Pdr18p, Pdr15p-Yer097wp, Ssm4p-Pdr18p and Bmh1p-Pxa2p) could not be tested by Co-IP due to technical issues associated with strain generation.



Supplementary Figure 13: Co-immunoprecipitation validation of ABC transporter interactions with Zrc1p and Zrt1p. Sizes indicated at top and bottom of boxes were estimated from MW markers on blots and are given in kDa. Rgt2p was used as a negative control.

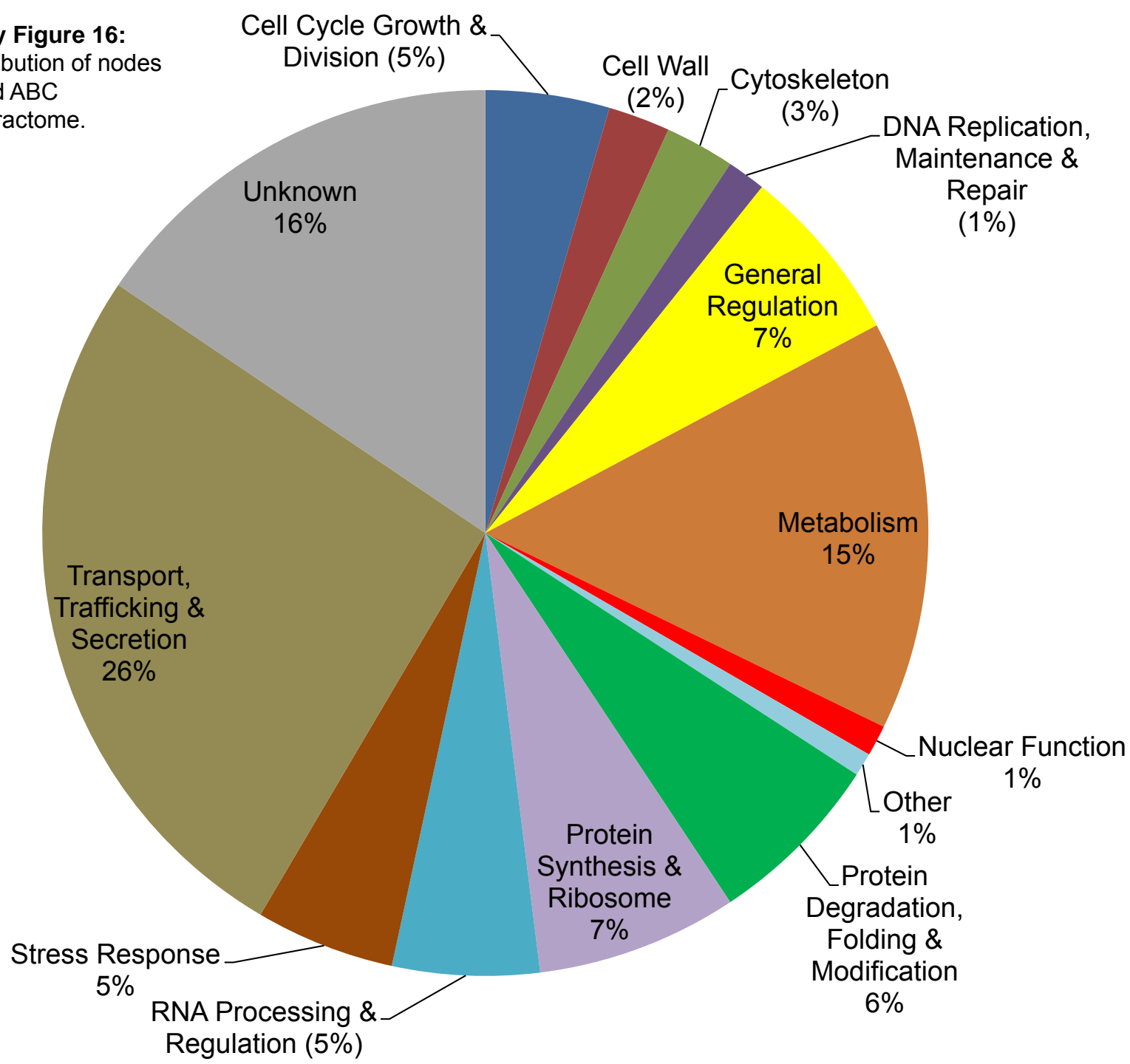


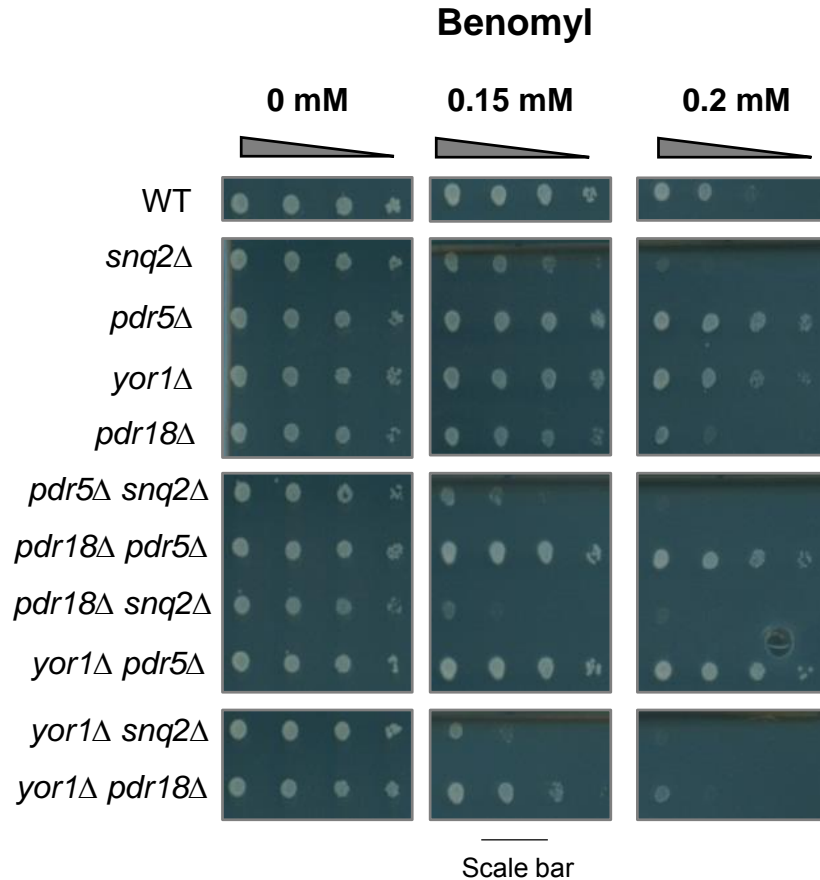
Supplementary Figure 14: Integrated ABC interactome showing conservation of proteins in humans and association with known human disease. Node color is used to indicate if a protein has a human ortholog (blue), has a human ortholog associated with human disease (red) or lacks an identifiable human ortholog (grey). Interactions between two proteins with a human ortholog are termed ‘conserved’ and are connected by lines colored to indicate if the interaction is unique to our MYTH screen (red line), previously reported but not detected by MYTH (yellow line) or previously reported and confirmed by our MYTH screen (blue line). Conserved interactions are connected by dashed lines if they have been experimentally validated in humans, or solid lines if they have not been experimentally validated in humans. Non-conserved interactions are connected by solid grey lines.



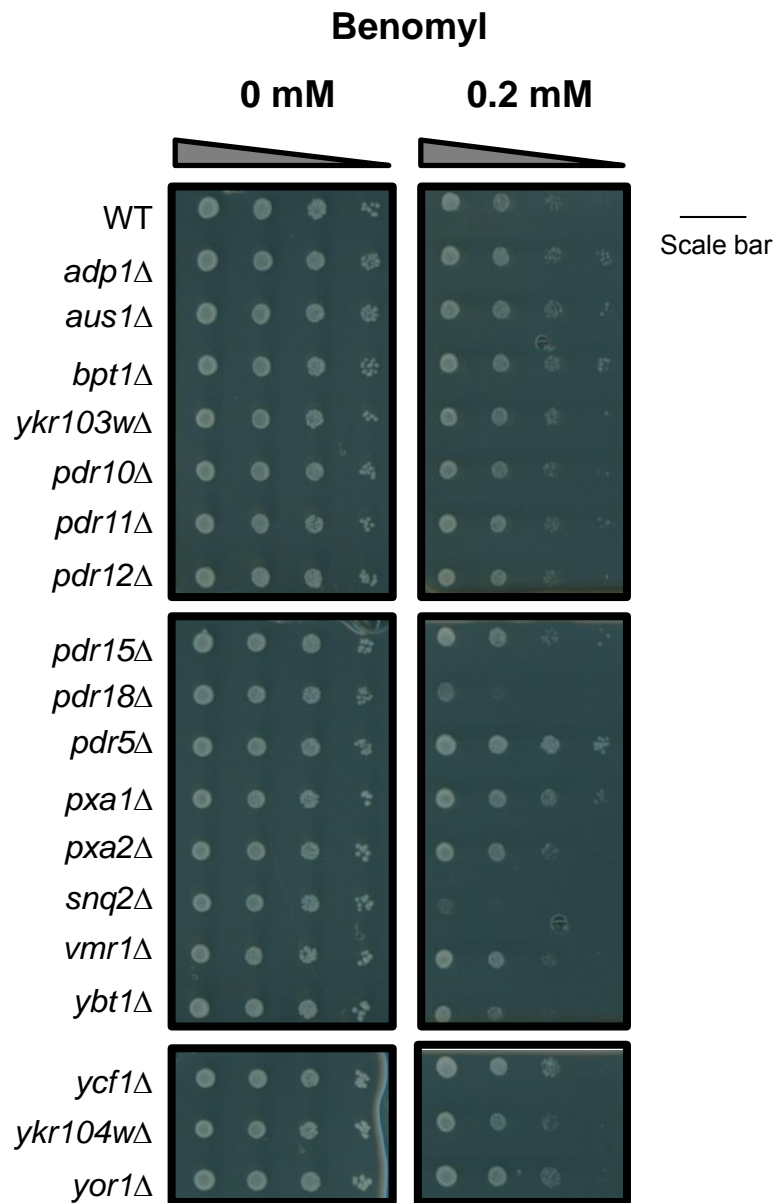
Supplementary Figure 15: ABC transporter interactome showing only interactions identified in our MYTH screen. Individual nodes are colored according to functional classification and are assigned a shape based on whether they are bait/prey and localized to the membrane or soluble fractions, as described in the legend.

Supplementary Figure 16:
Functional distribution of nodes
in the integrated ABC
transporter interactome.

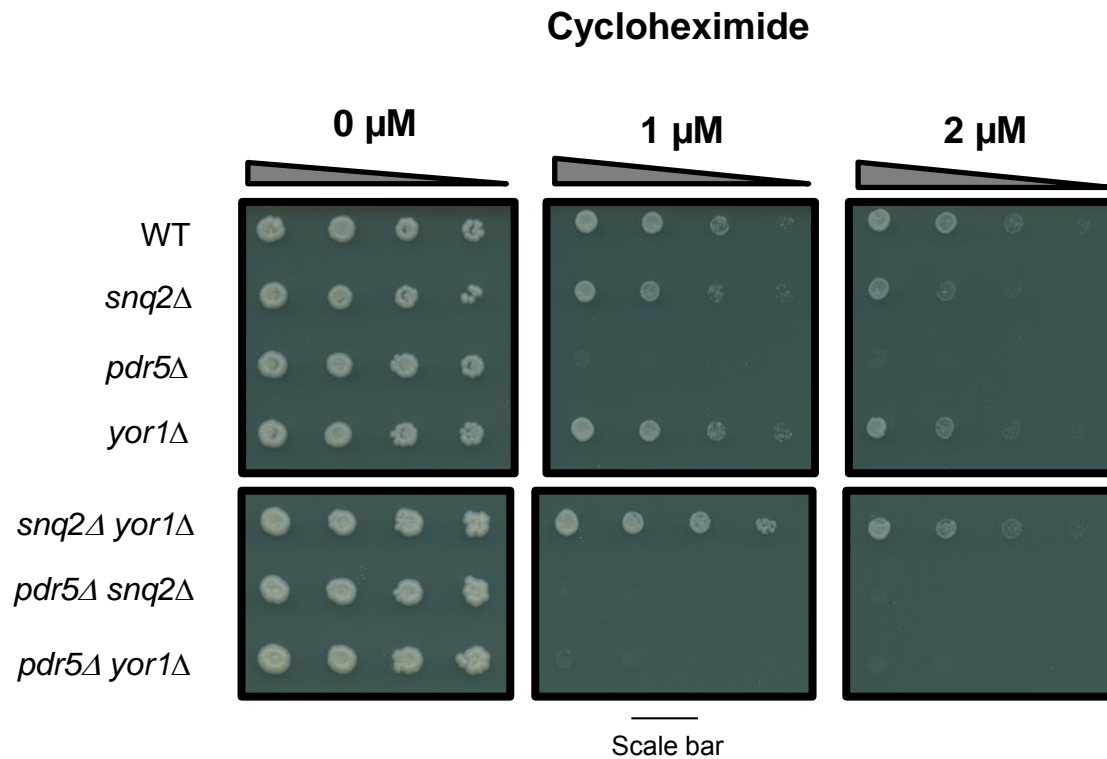




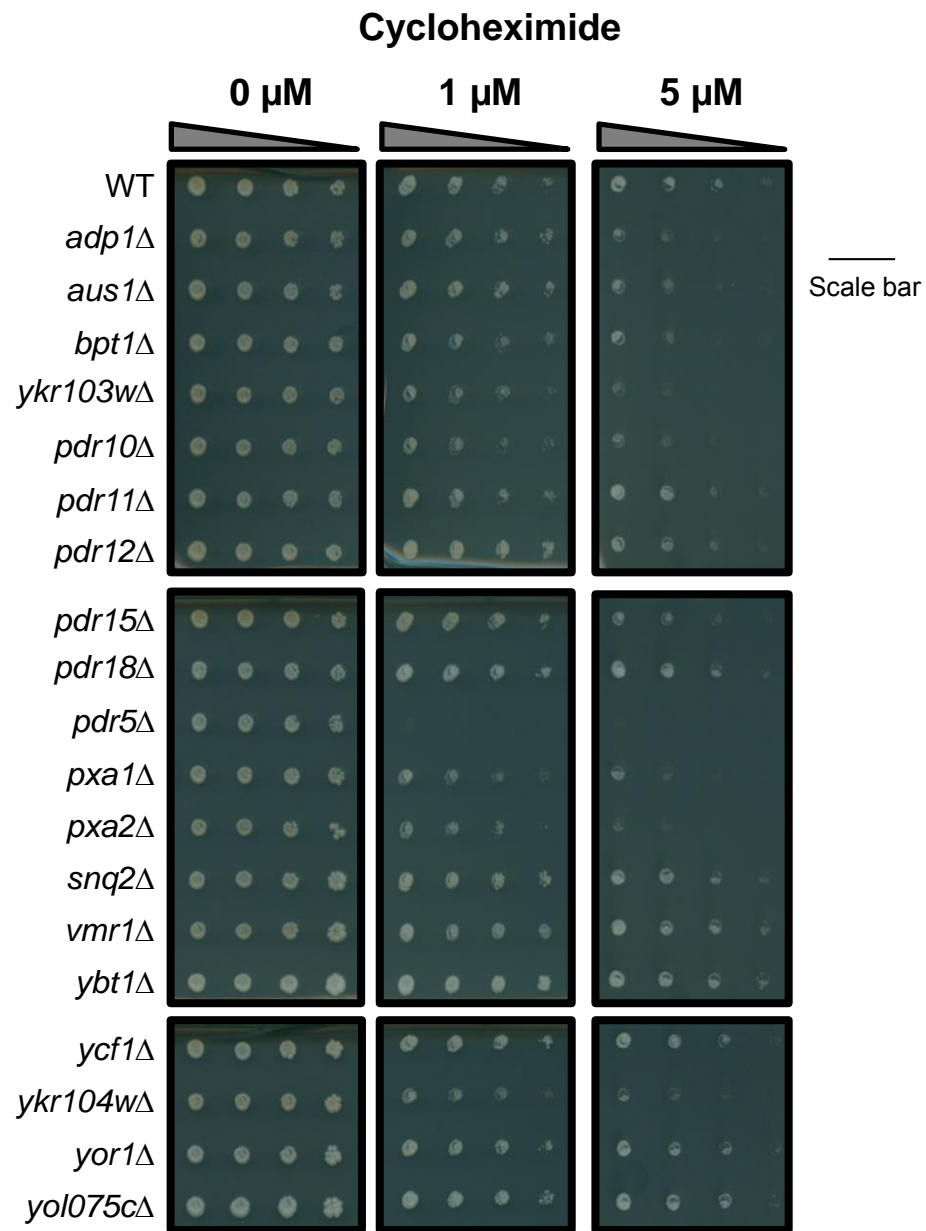
Supplementary Figure 17: Growth of ABC deletion strains challenged with the Snq2p transport substrate benomyl. Ten-fold serial dilutions of each strain were spotted onto SD-Complete media containing benomyl at the indicated concentrations and grown at 30°C for 3 days. Scale bar is 20 mm.



Supplementary Figure 18: Growth of ABC deletion strains challenged with the Snq2p transport substrate benomyl. Ten-fold serial dilutions of each strain were spotted onto SD-Complete media containing 0 or 0.2 mM benomyl and grown at 30°C for 3 days. Scale bar is 20 mm.

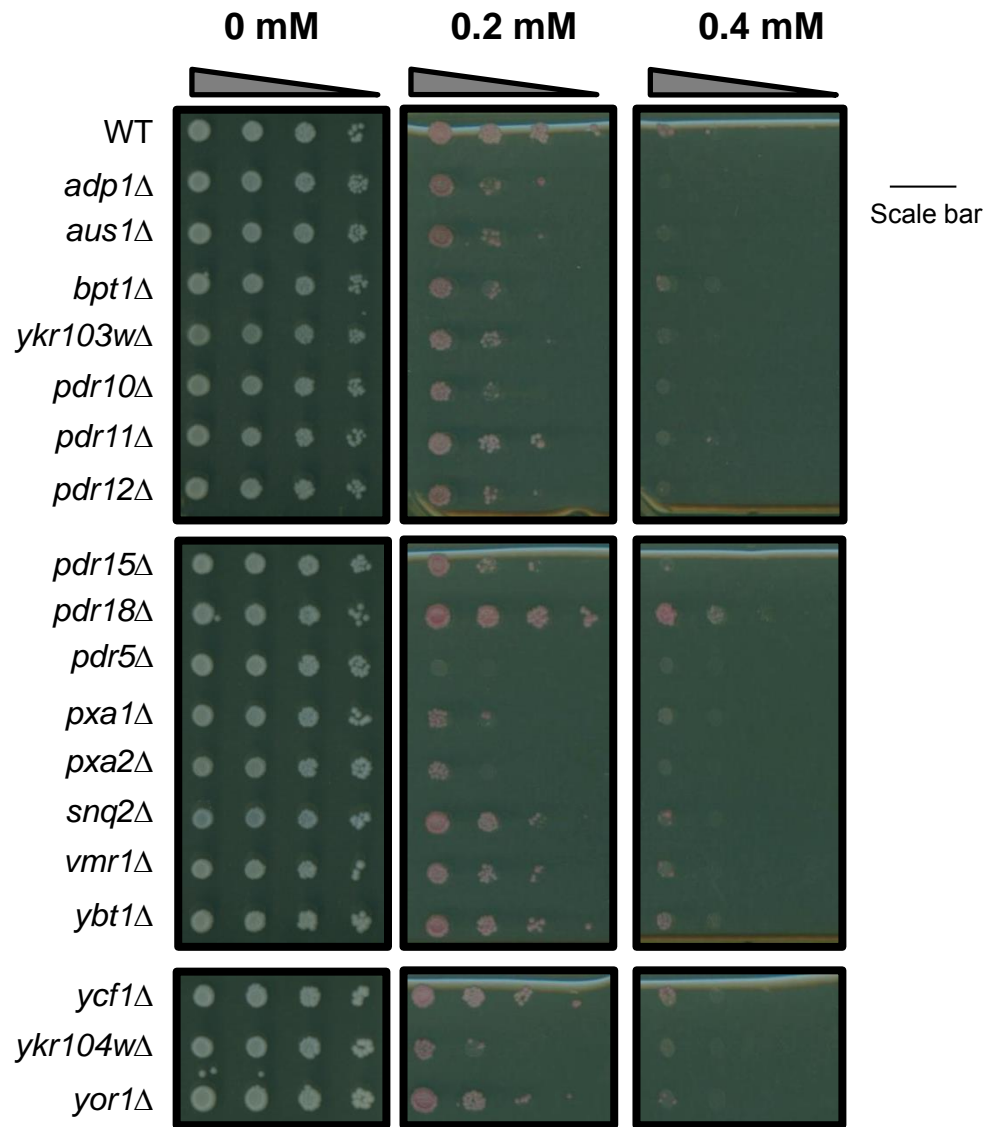


Supplementary Figure 19: Growth of selected ABC single and double deletion strains challenged with the Pdr5p transport substrate cycloheximide. Ten-fold serial dilutions of each strain were spotted onto SD-Complete media containing 0, 1 or 2 μM cycloheximide and grown at 30°C for 3 days. Scale bar is 15 mm.

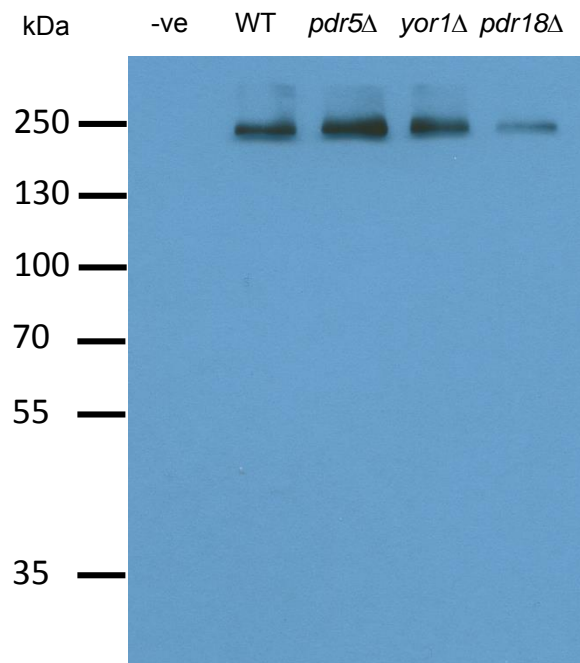


Supplementary Figure 20: Growth of ABC deletion strains challenged with the Pdr5p transport substrate cycloheximide. Ten-fold serial dilutions of each strain were spotted onto SD-Complete media containing 0, 1 or 5 μM cycloheximide and grown at 30°C for 3 days. Scale bar is 20 mm.

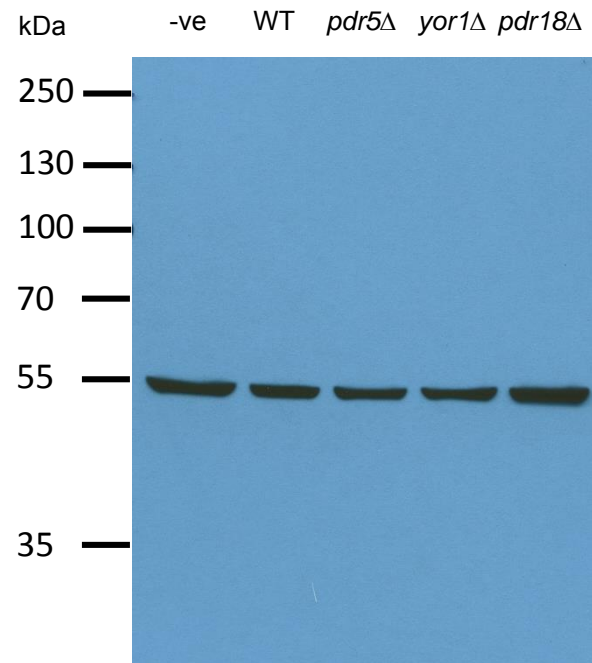
2,3,5-triphenyltetrazolium chloride (TTZ)



Supplementary Figure 21: Growth of ABC deletion strains challenged with the Pdr5p transport substrate 2,3,5-triphenyltetrazolium chloride (TTZ). Ten-fold serial dilutions of each strain were spotted onto SD-Complete media containing 0, 0.2 or 0.4 mM TTZ and grown at 30°C for 3 days. Scale bar is 15 mm.



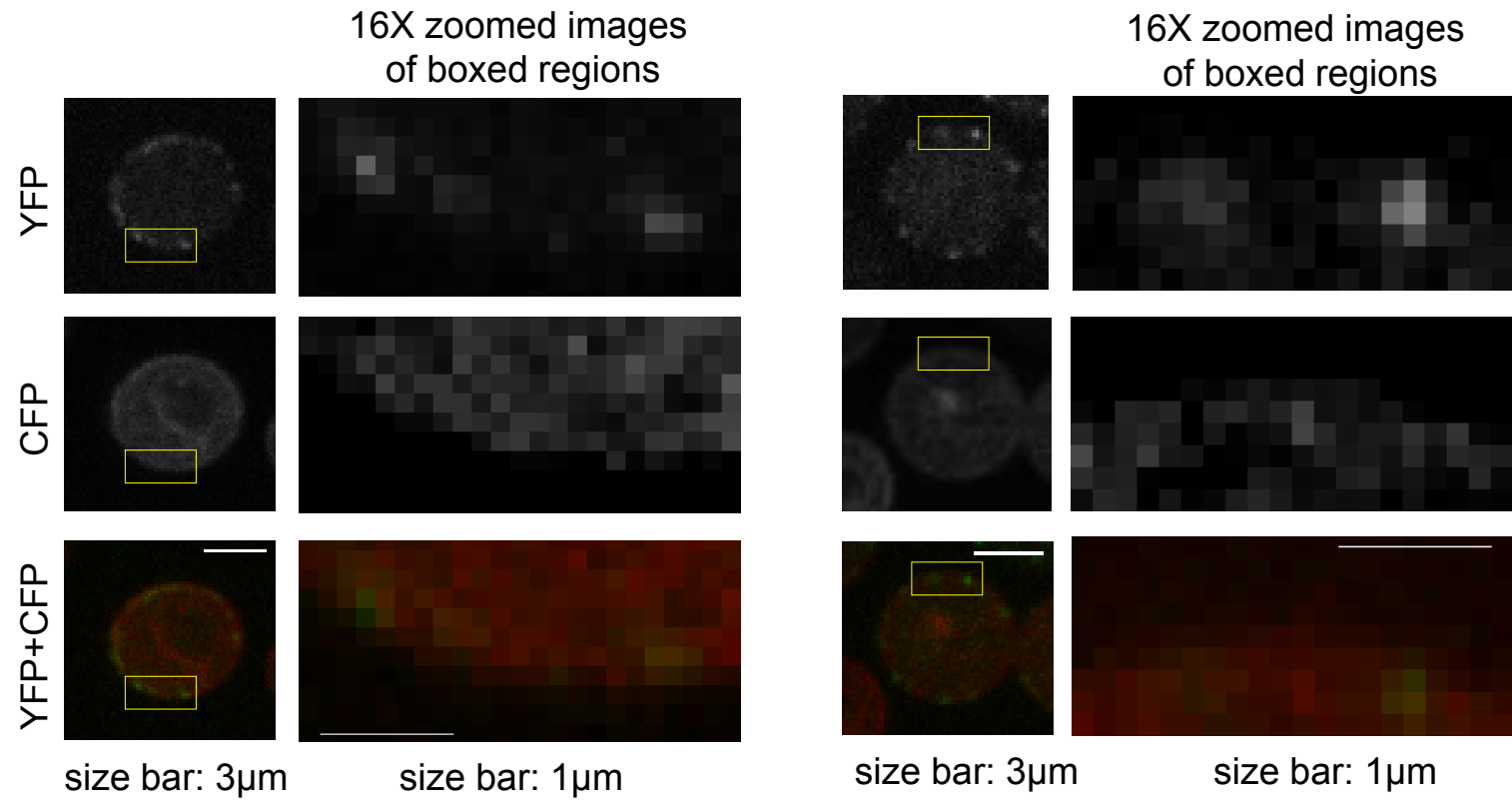
α-VP16
(Snq2p-CYT)



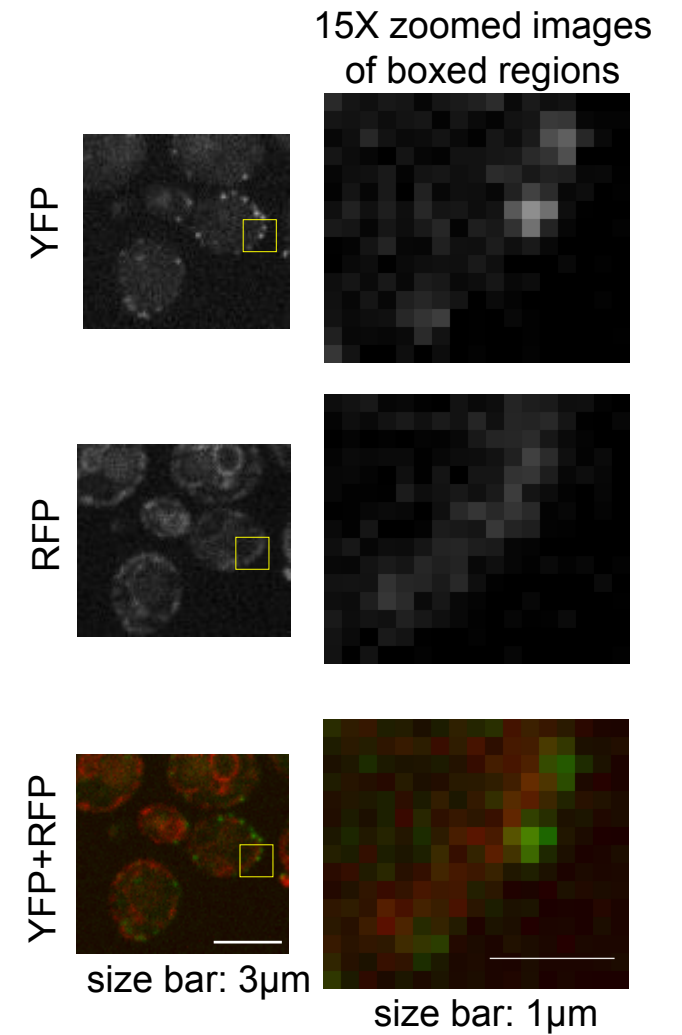
α-Hexokinase

Supplementary Figure 22: Full images of Snq2p-CYT and hexokinase control Western Blots.

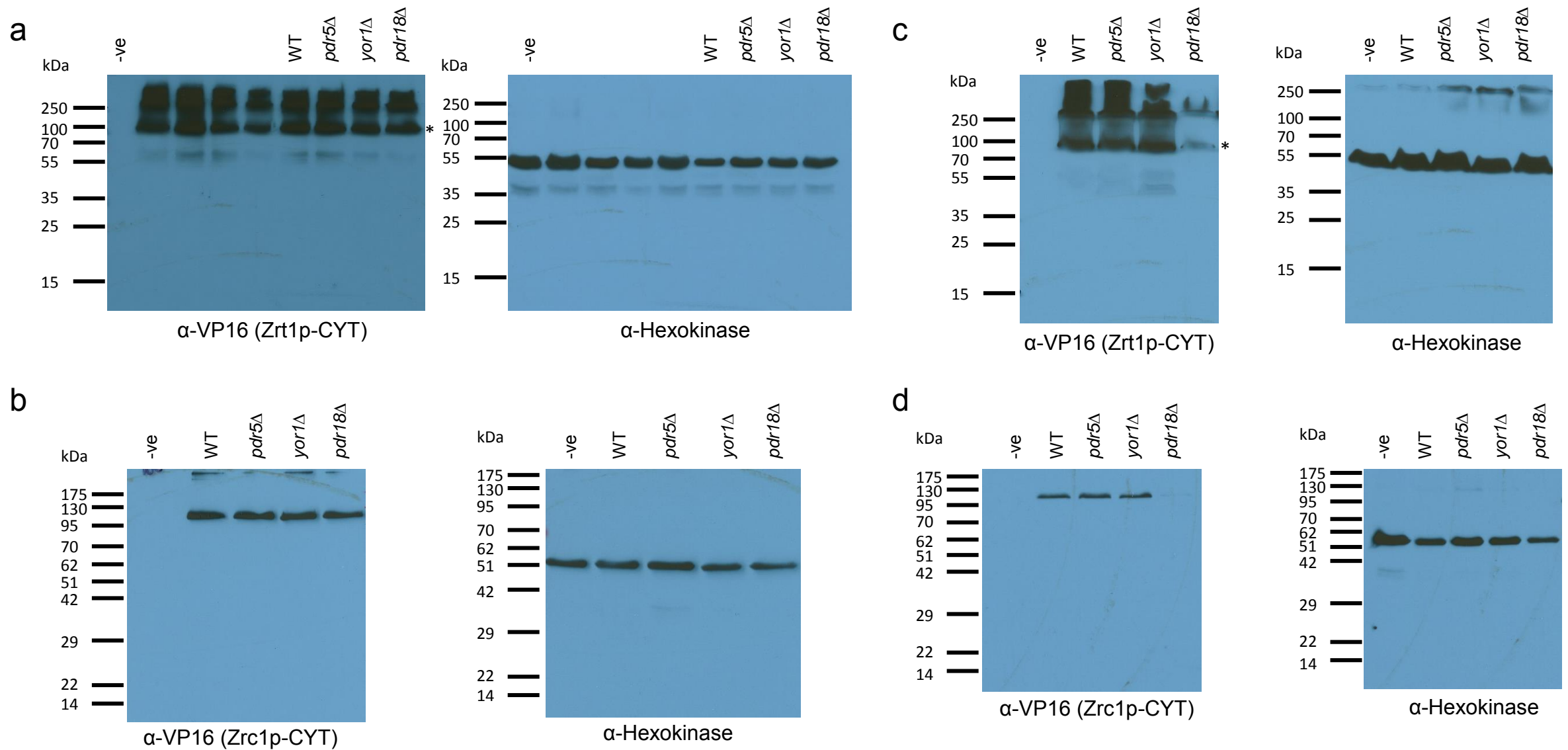
a



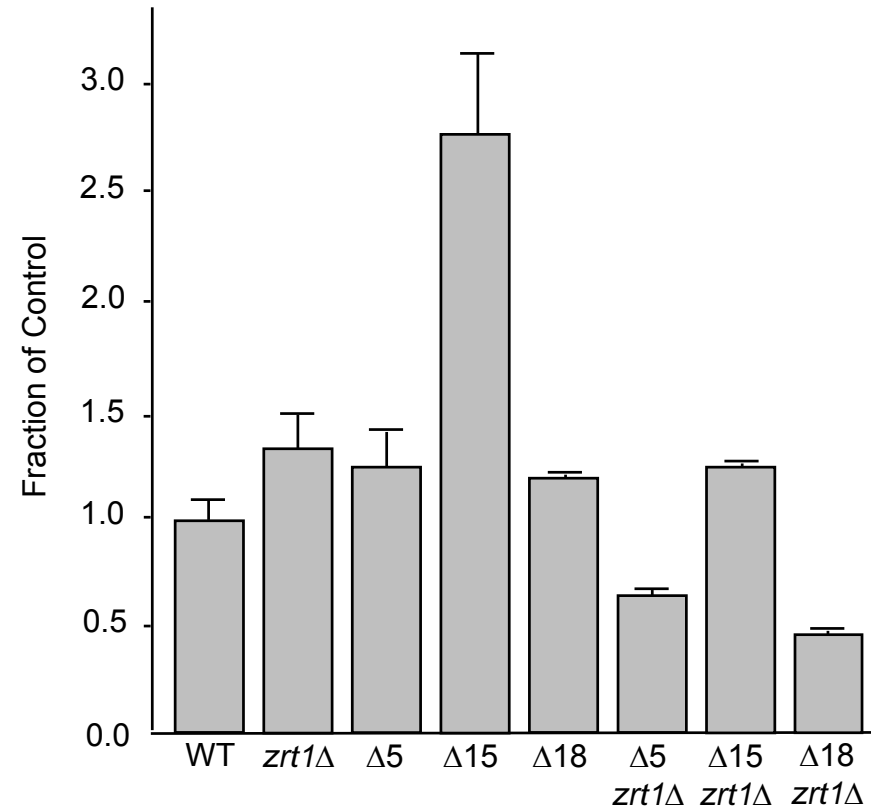
b



Supplementary Figure 23: Co-localization of the bimolecular fluorescent complex of VC-PDR10 and VN-ZRC1 with (a) the plasma membrane marker CFP-Cdc42 (2 views) and (b) the endoplasmic reticulum marker Sec63-mCherry. For YFP+CFP and YFP+RFP overlay images YFP signal is shown in Green, while CFP and RFP signals are shown in Red.



Supplementary Figure 24: Full images of Zrt1p-CYT, Zrc1p-CYT and hexokinase control Western Blots. (a) and (b) show blots performed on protein extracts from cells grown under conditions of zinc limitation. (c) and (d) show blots performed on protein extracts isolated from cells grown under zinc-replete conditions. Unlabelled lanes in (a) were not used in generation of figures. The '*' in (a) and (c) identify the bands presented in the cropped image.



Supplementary Figure 25: Analysis of zinc uptake in Y7092 WT and deletion strains. Values represent the average of three replicates (n=3) and are expressed relative to WT. Error bars indicate standard deviation. Zinc uptake is increased ~2.7 fold in the *pdr15*Δ strain relative to WT (two-tailed t-test, p-value = 1.6×10^{-3}), and decreased ~0.5 fold in *pdr5*Δ *zrt1*Δ (two-tailed t-test, p-value = 2.9×10^{-4}) and *pdr18*Δ *zrt1*Δ (two-tailed t-test, p-value = 6.5×10^{-5}) double deletion strains.

Supplementary Table 1: List of primers (shown 5' to 3') used in generation of iMYTH and tMYTH ABC transporter baits. Primer sequence in uppercase corresponds to ABC transporter gene-specific sequence.

Standard Name	Systematic Name	tMYTH / iMYTH	Tagging Primer Sequence
ADP1	YCR011C	tMYTH	F: <i>tcacacaatatttcaagctataccaagcatacaatcaactccaagcaacacaATGGGAAGTCATCGACGTTATC</i> R: <i>tcgacggtatcgataagcttgatcgattcctgcagatCTTTTGTTCACAACATCCAC</i>
AUS1	YOR011W	iMYTH	F: <i>ATCACCAAAAGTAATTCACACAGAGGGAAGAAGCCTGTACAGAAcAtgtcgggggggatccctcc</i> R: <i>GTTGTACAAAGGACTCTTTCAATTGTTTAGTCAGTCATTGGTGAcactataggagaccggcaga</i>
BPT1	YLL015W	tMYTH	F: <i>tcacacaatatttcaagctataccaagcatacaatcaactccaagcaacacaATGTCTTCACTAGAAGTGGTAG</i> R: <i>tcgacggtatcgataagcttgatcgattcctgcagatTTTCAAATACCCACCTTTCTC</i>
NFT1	YKR103W/YKR104W	tMYTH	A: <i>tcacacaatatttcaagctataccaagcatacaatcaactccaagcaacacaATGATAAAAAATGGTACATGCCCC</i> B: <i>CCCCGCTAGCCCCGCATCCAAATATGAGGCCTTCATTATGATC</i> C: <i>GATCATAATGAAGGCCTCATATTTGGATGCGGGGCTAGCGGGG</i> D: <i>tcgacggtatcgataagcttgatcgattcctgcagatCTTTTATTATCGAATGAGAC</i>
PDR10	YOR328W	tMYTH	F: <i>tcacacaatatttcaagctataccaagcatacaatcaactccaagcaacacaATGTTGCAAGCGCCCTCAAG</i> R: <i>tcgacggtatcgataagcttgatcgattcctgcagatTTTCTTTAATTTTTTGCCTTTTC</i>
PDR11	YIL013C	iMYTH	F: <i>ATGAGGCGGTCCAAAACATCTCATAATCCAAACGAACAAGCGTAatgtcgggggggatccctcc</i> R: <i>TCCGAAAAATGATTATAGATTAATTTAGAATATGATTTGGGAATAactataggagaccggcaga</i>
PDR12	YPL058C	iMYTH	F: <i>ATTTTCCAAACAGTTCAGGTGACGAAAATAAAATCACGAAGAAatgtcgggggggatccctcc</i> R: <i>ACTCACGAGTGGGATAGAAATGAAATCTTTTTCTTTTAAATGGTAactataggagaccggcaga</i>
PDR15	YDR406W	iMYTH	F: <i>AGGGTACCCAAGAAGAACGGTAAGATTTCCGAAAACCCAAGAAgAtgtcgggggggatccctcca</i> R: <i>CTATATAGAATATAGATAATATAAAAACGAAAAGAGCCTGATGTTGactataggagaccggcaga</i>
PDR18	YNR070W	tMYTH	F: <i>tcacacaatatttcaagctataccaagcatacaatcaactccaagcaacacaATGGAATGCGTTTCAGTAGAAG</i> R: <i>tcgacggtatcgataagcttgatcgattcctgcagatAATGAAACCGAAGTTTCTCCATAAG</i>
PDR5	YOR153W	iMYTH	F: <i>TGGTTAGCAAGAGTGCCTAAAAAGAACGGTAAACTCTCCAAGAAAatgtcgggggggatccctcca</i> R: <i>GATGCCTATAAAAAAAGTACCGATGAGATAACCTAGGAATAAAactataggagaccggcaga</i>
PXA1	YPL147W	iMYTH	F: <i>TGGGAAGATGAGAGGACGAAGCTACGGGAAAAGCTTGAATTTATatgtcgggggggatccctcca</i> R: <i>CGTGGATTCATCAAGTGAGATATATATATATATGTTTCATATTTGTactataggagaccggcaga</i>
PXA2	YKL188C	iMYTH	F: <i>TTGAACAAAAAAGTTAAAAACAAAAAGGAAGAAGGAAAGGAGAGGatgtcgggggggatccctcca</i> R: <i>AATTATATATAGGAAAGTGTATTTGCATAAAAAGGAAAAATAactataggagaccggcaga</i>
SNQ2	YDR011W	iMYTH	F: <i>GTATCTATACTCAATAAAATTAATAAACAATAAGGAAAAAGGAGCAgAtgtcgggggggatccctcca</i> R: <i>AAACTTTTTTACTCAACAAGACTTGACTTTTGAAAACACGAGAGactataggagaccggcaga</i>
STE6	YKL209C	iMYTH	F: <i>AATAATCGCGGGGAATTAATCCAAATTTGTTTCCAACCAAAGCAGTatgtcgggggggatccctcca</i> R: <i>GTCTCGAATATTTGAGTATGTTTTAGTTTTTTGTTTTATTTTTCactataggagaccggcaga</i>
VMR1	YHL035C	tMYTH	F: <i>tcacacaatatttcaagctataccaagcatacaatcaactccaagcaacacaATGGGAACGGATCCCCTTATTATC</i> R: <i>tcgacggtatcgataagcttgatcgattcctgcagatTTTCATCATCTTACTTGATT</i>
YBT1	YLL048C	iMYTH	F: <i>TTGGCTAAAAAGCCTTTGTGGAAAAATTGAACCTCTAAAAAGGACatgtcgggggggatccctcca</i> R: <i>ATTTATAGTACGTGAACATGTGTGCGTATATACATATATATATActataggagaccggcaga</i>
YCF1	YDR135C	iMYTH	F: <i>TTGTTCTATTCAGTGTGCATGGAGGCTGGTTTGGTCAATGAAAAatgtcgggggggatccctcca</i> R: <i>TAAGCCATTATCATCGTTGCCTTCATTATATCTTTTTATTGCTGactataggagaccggcaga</i>
YOL075C	YOL075C	tMYTH	F: <i>tcacacaatatttcaagctataccaagcatacaatcaactccaagcaacacaATGTCACAGCAGGAGAATGGTG</i> R: <i>tcgacggtatcgataagcttgatcgattcctgcagatCCATTTTATCCACTCCAATTT</i>
YOR1	YGR281W	iMYTH	F: <i>TGTTCTAGATCTGGTATTGTGGAAAATGATTTCCGAGAACAGAAGTatgtcgggggggatccctcca</i> R: <i>ATGTATAAATATATATTTCTAGAAATGAAAAGGACCGAAGCGCTTactataggagaccggcaga</i>

Supplementary Table 2: List of primers (shown 5' to 3') used in quantitative real time PCR experiments.

Standard Name	Systematic Name	F Primer	R Primer
ACT1	YFL039C	AGTGTGATGTCGATGTCCGT	TGACCTTCATGGAAGATGGA
SNQ2	YDR011W	CTTGTTGGTGAGGTTGGTTG	GGCCCATGAAGATTGAGAAT
ZRC1	YMR243C	AAAGCGGGAATAACGATTTG	GATTGTGGCAACACTTCACC
ZRT1	YGL255W	TCCTGCCATTATGCTAACGA	CAGCTGCAGTGTTTCTCACA